Supplementary Information for

Kinetic schemes for post-synchronized single molecule dynamics

Chunlai Chen, Michael J. Greenberg, Joseph M. Laakso, E. Michael Ostap,

Yale E. Goldman, and Henry Shuman

Step by step analysis on synchronized translocation traces.

Step 1: Add a reaction to complete the enzymatic cycle, to ensure nonzero steady state populations.

Since only the last state (POST) is populated in the steady state of the translocation scheme in Fig 2C is modified (Fig. S1) to include two reactions that complete the enzymatic cycle. The two introduced reactions are from the last state (POST) to PRE^C and PRE^H. In order to maintain the equilibrium concentrations of PRE^C and PRE^H in the absence of EF-G, the ratio of the new reaction rates k_{C3} and k_{H3} must be:

$$k_{C3} / k_{H3} = k_{-1} / k_{+1} \qquad \text{Eq. S1}$$

Step 2: solve the relative steady state concentrations analytically or numerically. The absolute concentrations are not needed; only ratios of the different states.

The steady state equations for scheme S1 are:

$$k_{C1}[PRE^C] + k_{-2}[PRE\text{-}G^H] = (k_{C2} + k_{+2})[PRE\text{-}G^C] \qquad \text{Eq. S2}$$

$$k_{H1}[PRE^H] + k_{+2}[PRE\text{-}G^C] = (k_{H2} + k_{-2})[PRE\text{-}G^H] \qquad \text{Eq. S3}$$

$$k_{C3}[POST] + k_{-1}[PRE^H] = (k_{C1} + k_{+1})[PRE^C] \qquad \text{Eq. S4}$$

$$k_{H3}[POST] + k_{+1}[PRE^C] = (k_{H1} + k_{-1})[PRE^H] \qquad \text{Eq. S5}$$

The concentration ratios formed from the steady state solutions of Eq. S1-5, which are essential for calculating reversed rates are:

$$\frac{[PRE^C]}{[PRE^H]} = (k_{-1}\,(k_{+1} + k_{H1} + k_{-1})) / (k_{+1}\,(k_{C1} + k_{+1} + k_{-1})) \qquad \text{Eq. S6}$$

$$\frac{[PRE^C]}{[PRE\text{-}G^C]} = (k_{-1}\,(k_{+1} + k_{H1} + k_{-1})\,(k_{+2}\cdot k_{H2} + k_{C2}\,(k_{H2} + k_{-2}))) / (k_{C1}\cdot k_{-1}\,(k_{+1} + k_{H1} + k_{-1})\,k_{H2} + (k_{+1} +$$

$$k_{-1})\,(k_{+1}\cdot k_{H1} + k_{C1}\,(k_{H1} + k_{-1}))\,k_{-2}) \qquad \text{Eq. S7}$$

$$\frac{[PRE^H]}{[PRE\text{-}G^H]} = (k_{+1}\,(k_{C1} + k_{+1} + k_{-1})\,(k_{+2}\cdot k_{H2} + k_{C2}\,(k_{H2} + k_{-2}))) / (k_{+1}\,k_{H1}\,(k_{C1} + k_{+1} + k_{-1})\,k_{C2} + (k_{+1} +$$

$$k_{-1})\,(k_{+1}\cdot k_{H1} + k_{C1}\,(k_{H1} + k_{-1}))\,k_{+2}) \qquad \text{Eq. S8}$$

$$\frac{[PRE\text{-}G^H]}{[PRE\text{-}G^C]} = (k_{+1}\cdot k_{H1}\,(k_{C1} + k_{+1} + k_{-1})\,k_{C2} + (k_{+1} + k_{-1})\,(k_{+1}\cdot k_{H1} + k_{C1}\,(k_{H1} + k_{-1}))\,k_{+2}) / (k_{C1}\cdot k_{-1}\,(k_{+1} +$$

$k_{H1} + k_{-1})\ k_{H2} + (k_{+1} + k_{-1})\ (k_{+1}\cdot k_{H1} + k_{C1}\ (k_{H1} + k_{-1}))\ k_{-2})$ Eq. S9

Note that these ratios are independent of the introduced reaction rates k_{C3} and k_{H3}.

Step 3: Calculate the transition rates for time reversed scheme.
The time-reversed rates in Fig. 2D as calculated from Eq. 3 (of the main text) are:

$$k'_{C1} = k_{C1}\frac{[\text{PRE}^{C}]}{[\text{PRE-G}^{C}]} = k_{C1}\,(k_{-1}\ (k_{+1} + k_{H1} + k_{-1})\ (k_{+2}\cdot k_{H2} + k_{C2}\ (k_{H2} + k_{-2}))) \,/\, (k_{C1}\cdot k_{-1}\ (k_{+1} + k_{H1} + k_{-1})$$

$k_{H2} + (k_{+1} + k_{-1})\ (k_{+1}\cdot k_{H1} + k_{C1}\ (k_{H1} + k_{-1}))\ k_{-2})$ Eq. S10

$$k'_{H1} = k_{H1}\frac{[\text{PRE}^{H}]}{[\text{PRE-G}^{H}]} = k_{H1}\,(k_{+1}\ (k_{C1} + k_{+1} + k_{-1})\ (k_{+2}\cdot k_{H2} + k_{C2}\ (k_{H2} + k_{-2}))) \,/\, (k_{+1}\ k_{H1}\ (k_{C1} + k_{+1} + k_{-1})$$

$k_{C2} + (k_{+1} + k_{-1})\ (k_{+1}\cdot k_{H1} + k_{C1}\ (k_{H1} + k_{-1}))\ k_{+2})$ Eq. S11

$$k'_{+1} = k_{+1}\frac{[\text{PRE}^{C}]}{[\text{PRE}^{H}]} = k_{+1}\,(k_{-1}\ (k_{+1} + k_{H1} + k_{-1})) \,/\, (k_{+1}\ (k_{C1} + k_{+1} + k_{-1}))$$ Eq. S12

$$k'_{-1} = k_{-1}\frac{[\text{PRE}^{H}]}{[\text{PRE}^{C}]} = k_{-1}\,(k_{+1}\ (k_{C1} + k_{+1} + k_{-1})) \,/\, (k_{-1}\ (k_{+1} + k_{H1} + k_{-1}))$$ Eq. S13

$$k'_{+2} = k_{+2}\frac{[\text{PRE-G}^{C}]}{[\text{PRE-G}^{H}]} = k_{+2}\,(k_{C1}\cdot k_{-1}\ (k_{+1} + k_{H1} + k_{-1})\ k_{H2} + (k_{+1} + k_{-1})\ (k_{+1}\cdot k_{H1} + k_{C1}\ (k_{H1} + k_{-1}))\ k_{-2}) \,/$$

$(k_{+1}\cdot k_{H1}\ (k_{C1} + k_{+1} + k_{-1})\ k_{C2} + (k_{+1} + k_{-1})\ (k_{+1}\cdot k_{H1} + k_{C1}\ (k_{H1} + k_{-1}))\ k_{+2})$ Eq. S14

$$k'_{-2} = k_{-2}\frac{[\text{PRE-G}^{H}]}{[\text{PRE-G}^{C}]} = k_{-2}\,(k_{+1}\cdot k_{H1}\ (k_{C1} + k_{+1} + k_{-1})\ k_{C2} + (k_{+1} + k_{-1})\ (k_{+1}\cdot k_{H1} + k_{C1}\ (k_{H1} + k_{-1}))\ k_{+2}) \,/$$

$(k_{C1}\cdot k_{-1}\ (k_{+1} + k_{H1} + k_{-1})\ k_{H2} + (k_{+1} + k_{-1})\ (k_{+1}\cdot k_{H1} + k_{C1}\ (k_{H1} + k_{-1}))\ k_{-2})$ Eq. S15

Step 4: Treat the averaged trajectory before the trigger point as a "time-reversed" perturbation experiment and extract its kinetics using the time-reversed rate constants

The experimental rates, $k_{C\text{-sync}}$ and $k_{H\text{-sync}}$, fitted from synchronized traces in Fig. 2B are eigenvalues of reversed reaction scheme (Fig. 2D):

$$\frac{1}{2}\left(k'_{C1}+k'_{H1}+k'_{+2}+k'_{-2}+\sqrt{(k'_{C1}+k'_{H1}+k'_{+2}+k'_{-2})^2\text{-}4\ (k'_{C1}\ k'_{H1}+k'_{C1}\ k'_{+2}+k'_{H1}\ k'_{-2})}\right) = \max(k_{C\text{-sync}}, k_{H\text{-sync}})$$

Eq. S16

$$\frac{1}{2}\left(k'_{C1}+k'_{H1}+k'_{+2}+k'_{-2}\text{-}\sqrt{(k'_{C1}+k'_{H1}+k'_{+2}+k'_{-2})^2\text{-}4\ (k'_{C1}\ k'_{H1}+k'_{C1}\ k'_{+2}+k'_{H1}\ k'_{-2})}\right) = \min(k_{C\text{-sync}}, k_{H\text{-sync}})$$

Eq. S17

k_{+1}, k_{-1}, k_{C2}, k_{H2}, $k_{C\text{-}sync}$, and $k_{H\text{-}sync}$ are experimentally measured rates determined in our previous study (1). At 2 μM EF-G, values of both k_{C1} and k_{H1} are set to 100 s^{-1} based on the previously reported EF-G binding rate (2). Combining and simplifying Eqs. S10-17 using the known values of k_{+1}, k_{-1}, k_{C2}, k_{H2}, $k_{C\text{-}sync}$, $k_{H\text{-}sync}$, k_{C1}, and k_{H1}, leads to two independent equations and two unknowns, k_{+2} and k_{-2}, the transition rates between classical and hybrid PRE states after EF-G binding. The resulting values of k_{+2} and k_{-2} for three different types of ribosome complexes (Table S1) are, in all cases, not significantly different from zero and smaller than k_{+1} and k_{-1}. These results indicate that EF-G binding suppresses transitions between the classical and hybrid PRE states prior to translocation. In a homogeneous system, the two synchronized traces in Fig. 2B are expected to extrapolate back to the same value. Due to heterogeneity of the sample discussed previously (1, ribosomes translocating from the classic and hybrid states are apparently different), the back extrapolations of two traces do not meet.

Table S1 Reaction rates for translocation examples.

Complex	Experimental data (s^{-1}) [a]						calculated from model (s^{-1}) [b]	
	k_{C2}	$k_{C\text{-}sync}$	k_{H2}	$k_{H\text{-}sync}$	k_{+1}	k_{-1}	k_{+2}	k_{-2}
PRE-I-Lt	0.31±0.06	0.37±0.07	0.13±0.04	0.14±0.02	0.59±0.06	0.77±0.05	0.057±0.072	0.013±0.049
PRE-II-Lt	0.30±0.03	0.48±0.11	0.36±0.05	0.32±0.04	0.56±0.05	0.73±0.10	0.06±0.12	0.08±0.09
PRE-II-tt	0.25±0.06	0.31±0.05	0.68±0.03	0.83±0.13	0.59±0.04	0.67±0.06	0.08±0.09	0.13±0.10

[a] Experimental data are from our previous study (1).

[b] k_{C1} = 100 s^{-1} and k_{H1} = 100 s^{-1} are used based previous study (2).

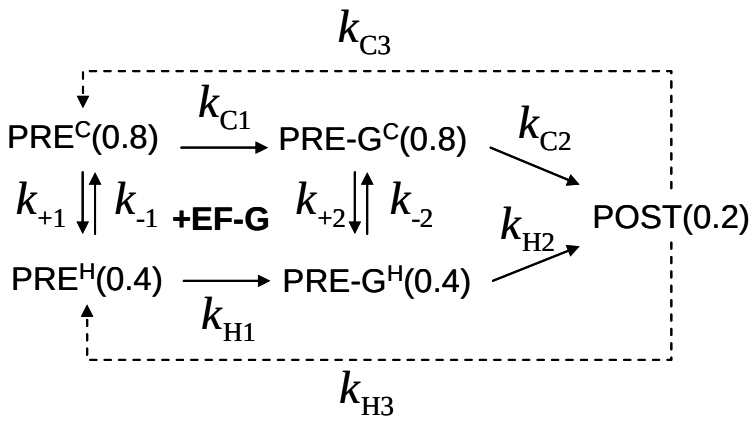

Fig. S1 Forward scheme of translocation with introduced reactions (dash lines) to produce non-zero steady state populations. The introduced reactions are from the last state to the first state (equilibrium between PRE^{C} and PRE^{H} in the absence of EF-G), which satisfies Eq. S1.

REFERENCES:

1. Chen, C., B. Stevens, J. Kaur, D. Cabral, H. Liu, Y. Wang, H. Zhang, G. Rosenblum, Z. Smilansky, Y. E. Goldman, and B. S. Cooperman. 2011. Single-Molecule Fluorescence Measurements of Ribosomal Translocation Dynamics. Mol cell 42:367-377.
2. Savelsbergh, A., V. I. Katunin, D. Mohr, F. Peske, M. V. Rodnina, and W. Wintermeyer. 2003. An elongation factor G-induced ribosome rearrangement precedes tRNA-mRNA translocation. Mol Cell 11:1517-1523.